Noise, ill-conditioning and sensor placement analysis for force estimation through virtual sensing

T.Tamarozzi [1,2], **E.Risaliti** [1,2], **W. Rottiers** [2,3], **K. Janssens** [1], **W. Desmet** [2,3]

[1] Siemens Industry Software NV,
Interleuvenlaan 68, B-3001 Leuven, Belgium
e-mail: **tommaso.tamarozzi@siemens.com**

[2] KU Leuven, Department of Mechanical Engineering,
Celestijnenlaan 300 B, B-3001, Heverlee, Belgium

[3] Member of Flanders Make

Abstract

The knowledge of loads acting on machines and components is crucial in many application fields. Input estimation though is a very challenging inverse problem with which researchers have struggled over the last decades. Several issues related to ill-conditioning and ill-posedness are not sufficiently understood nor solved. This paper proposes an in-depth numerical study covering some of the aspects that can make the difference between a reliable and an unreliable force estimation. A states-input estimation algorithm for multiple force estimation is implemented as a linear augmented Kalman filter/smoother coupled with a reduced order model of a complex ill-posed mechanical structure, namely a twistbeam rear suspension. The influence of different noise levels, measurements scaling and time horizon used for the estimation is thoroughly analyzed. Finally, an observability-based optimal sensors placement strategy is implemented showing robustness improved accuracy of the estimated quantities.

1 Introduction

The knowledge of external input forces acting on machines or components is crucial in many application fields. In particular the automotive, aerospace and manufacturing industries can largely benefit from this knowledge in order to improve their design process and increase the reliability and lifetime of their products. Thanks to the accurate prediction of loads and deformations of components/systems, several tasks that are essential in modern machines can be performed in a faster and more accurate way: precise control of actuators, reliable estimation of remaining lifetime, motion and deformation prediction, vibration analysis, etc... Standard methods to measure loads or quantities linked to system states directly (e.g. deformation, strain, velocity, acceleration fields) suffer from several drawbacks that oftentimes largely limit their performances. In particular force cells can be expensive, difficult to mount and are usually intrusive to the structure, therefore modifying the transfer path between input and output locations. Accelerometers, position and strain sensors, are generally trustworthy and accurate but provide only local information. Would one be interested in the full - strain/acceleration/displacement - fields to e.g. detect failure prone areas, then an unreasonable number of sensors and acquisition channels would be needed.

Force estimation is a very challenging inverse problem with which researchers have struggled over the last decades [1–4]. This is true regardless the linear or non-linear behavior of the structure, meaning that potential

non-linearities are likely to make the problem even more challenging but linear systems present their fare share of complications. Despite the importance of the topic, several issues related to ill-conditioning and ill-posedness are not sufficiently understood nor solved. Hybrid methods combining test-based and model-based strategies have the potential to merge the benefits of the two worlds and at least reduce the influence of ill-conditioning and ill-posedness to a minimum.

This work is not meant to provide a rigorous solution to the above mentioned problems but analyzes in details several factors that contributes to the failure of input-state estimation techniques in the field of (linear) structural dynamics with a particular focus towards multiple force estimation. Solutions such as increasing the estimation horizon, improving sensors accuracy and an optimal sensor placement strategy are analyzed and presented with engineering eyes. The paper is structured as follows: first the theory behind three popular methods for input-states estimation is briefly reviewed, namely Linear Least Squares (LLS), Augmented Kalman Filtering (AKF) and Augmented Kalman Smoothing (AKS). Afterward some experimental and numerical examples that allow to highlight the problems caused by ill-conditioning and ill-posedness are proposed. The following section analyzes the influence of sensors location, accuracy and horizon length on the estimation quality in a LLS setting is presented. Before the closing remarks, a section introduces an optimal sensor placement strategy and shows by means of numerical examples how such a strategy can be beneficial when combined with accurate sensors and longer estimation horizons.

2 Brief Theory: Linear Least Square and Augmented Kalman Filter/smoother for structural dynamics systems

In this section a brief overview of three popular methods for force estimation is given:

- Linear Least Squares;
- Augmented Kalman Filter;
- Augmented Kalman Smoother.

It has to be underlined that the conclusions drawn during the paper are general in nature and apply to most of the time-domain methods for states-input estimation.

Lets introduce first some general notation about second order structural dynamics systems including notions of reduced order models. The continuous time equations of motion can be written as

$$\mathbf{M}_z\ddot{\mathbf{z}}(t) + \mathbf{C}_z\dot{\mathbf{z}}(t) + \mathbf{K}_z\mathbf{z}(t) = \mathbf{B}_z\mathbf{u}(t) \tag{1}$$

where $\mathbf{z} \in \mathbb{R}^{n_{dof}}$ is the vector of the displacement Degrees of Freedom (DOFs) of the system (with n_{dof} the number of DOFs) and $\mathbf{u} \in \mathbb{R}^{n_i}$ is the input vector (with n_i the number of inputs). $\mathbf{M}_z$, $\mathbf{C}_z$ and $\mathbf{K}_z$ are the mass, damping and stiffness matrices and $\mathbf{B}_z$ is the input Boolean matrix, while t is the time variable. When using the Finite Element Method (FEM) [5], Model Order Reduction (MOR) [6] can be used in order to reduce the size of the Finite Element Model of the system, hence improving computational efficiency. A multitude of methods exist in literature to select an appropriate reduction space for the problem at hand. The following reduction basis is used in this work

$$\mathbf{\Psi} = \begin{bmatrix} \mathbf{\Psi}_{ram} & \mathbf{\Psi}_{nm} \end{bmatrix} \tag{2}$$

where $\mathbf{\Psi}_{ram} \in \mathbb{R}^{n_{dof} \times n_{inp}}$ is the matrix of so-called *residual attachment modes* [7] and $\mathbf{\Psi}_{nm} \in \mathbb{R}^{n_{dof} \times n_{nm}}$ is a matrix containing a limited number of eigenmodes of the structure. The enrichment of the reduction basis with residual attachment modes allows to have an exact (in a FE sense) representation of the static

response of the structure in response to loads applied at the selected input locations. The $\mathbf{z}$ vector of the DOFs can be approximated by means of the following equation:

$$\mathbf{z} \simeq \mathbf{\Psi q} \tag{3}$$

where the vector $\mathbf{q} \in \mathbb{R}^{n_{red}}$ contains the reduced coordinates of the system, with $n_{red} = n_{ram} + n_{nm}$ and $n_{red} \ll n_{dof}$. The reduced equations of motion, projected on to the reduction space can be written by direct substitution of Eq.(3) into Eq.(1) and by projecting the latter onto the reduction basis $\mathbf{\Psi}$, hence obtaining

$$\mathbf{M}_r\ddot{\mathbf{q}}(t) + \mathbf{C}_r\dot{\mathbf{q}}(t) + \mathbf{K}_r\mathbf{q}(t) = \mathbf{B}_r\mathbf{u}(t) \tag{4}$$

where $\mathbf{M}_r$, $\mathbf{C}_r$, $\mathbf{K}_r$ and $\mathbf{B}_r$ are the mass, damping, stiffness and input shape matrix of the reduced system. It is oftentimes useful to re-write Eq.(4) in state space form to benefit from the numerous available time integrators and estimators that are developed for first-order systems. By starting from Eq.(4) and by defining the state vector $\mathbf{x} \in \mathbb{R}^{n_s}$, with n_s the number of states, as

$$\mathbf{x} = \begin{bmatrix} \mathbf{q} \\ \dot{\mathbf{q}} \end{bmatrix}, \tag{5}$$

the state space equations of motion, also called *model equation*, complemented with the *measurement equation* can be written as

$$\begin{cases} \dot{\mathbf{x}}(t) = \mathbf{A}\mathbf{x}(t) + \mathbf{B}\mathbf{u}(t) \\ \mathbf{y}(t) = \mathbf{C}\mathbf{x}(t) + \mathbf{D}\mathbf{u}(t). \end{cases} \tag{6}$$

In Eq.(6), $\mathbf{y} \in \mathbb{R}^{n_o}$ is the output vector (or measurements vector) with n_o the number of outputs and $\mathbf{A}$, $\mathbf{B}$, $\mathbf{C}$ and $\mathbf{D}$ are real matrices of appropriate dimensions. The definition of matrices $\mathbf{C}$ and $\mathbf{D}$ depends on the type of measurements that are collected in the output vector $\mathbf{y}$, see e.g. [8] and the FE discretization used. Position, strain and acceleration measurements are considered in this work. Only acceleration measurements present a feed-through term involving the usage of matrix $\mathbf{D}$. For time simulation, Eq.(6) needs to be discretized as follows:

$$\begin{cases} \mathbf{x}_k &= \mathbf{F}\mathbf{x}_{k-1} + \mathbf{G}\mathbf{u}_{k-1} \\ \mathbf{y}_k &= \mathbf{H}\mathbf{x}_k + \mathbf{L}\mathbf{u}_k \end{cases} \tag{7}$$

where the computation of matrices $\mathbf{F}$, $\mathbf{G}$, $\mathbf{H}$, $\mathbf{L}$ depends on the choice of the discretization scheme. Details about this can be found in e.g. [9].

2.1 Linear Least Squares

Linear Least Square (LLS) is a common method that has been the subject of a very large number of studies, see e.g. [10]. It is used as a standard method in inverse problems. In this work, the LLS approach is used to infer input forces from measurements. The LLS method will be used only to highlight some peculiar properties of inverse problems and force estimation with respect to amount of sensors, noise levels and estimation horizon length. Without loss of generality, if acceleration measurements are not used, the measurement equation can be re-written, for multiple time steps as:

$$\begin{bmatrix} \mathbf{y}_1 \\ \mathbf{y}_2 \\ \dots \\ \mathbf{y}_k \end{bmatrix} - \begin{bmatrix} \mathbf{HF} \\ \mathbf{HF}^2 \\ \dots \\ \mathbf{HF}^k \end{bmatrix} \mathbf{x}_0 = \begin{bmatrix} \mathbf{HG} & \mathbf{0} & \dots & \mathbf{0} \\ \mathbf{HFG} & \mathbf{HG} & \dots & \mathbf{0} \\ \dots & \dots & \dots & \dots \\ \mathbf{HF}^{k-1}\mathbf{G} & \mathbf{HF}^{k-2}\mathbf{G} & \dots & \mathbf{HG} \end{bmatrix} \begin{bmatrix} \mathbf{u}_0 \\ \mathbf{u}_1 \\ \dots \\ \mathbf{u}_{k-1} \end{bmatrix} \tag{8}$$

where the subscript *k* represents a time-step and $\mathbf{x}_0$ is the vector of known initial conditions. Equation (8) can be re-written in matrix notation as:

$$\mathbf{Y} - \mathbf{I_0} = \tilde{\mathbf{F}}\mathbf{U} \tag{9}$$

where $\mathbf{Y} \in \mathbb{R}^{n_o \cdot k}$ is the vector of measured quantities across several time-steps, $\mathbf{I}_0$ represents the influence of the initial conditions across several time-steps, $\tilde{\mathbf{F}} \in \mathbb{R}^{n_o \cdot k \times n_i \cdot k}$ is the system matrix and $\mathbf{U} \in \mathbb{R}^{n_i \cdot k}$ is the input vector. If the number of sensors is larger than the number of input forces to be estimated and if the measurement equations are linearly independent (such that matrix $\tilde{\mathbf{F}}$ has at least rank $n_i \cdot k$), the system of equation (9) is overdetermined and can be solved in a least-square sense for $\mathbf{U}$ by e.g. using a Moore-Penrose pseudoinverse of matrix $\tilde{\mathbf{F}}$. Finally if the force to be estimated is slowly varying in time or even constant, matrix $\tilde{\mathbf{F}}$ and $\mathbf{U}$ become:

$$\tilde{\mathbf{F}} = \begin{bmatrix} \mathbf{HG} \\ \mathbf{HFG} + \mathbf{HG} \\ \dots \\ \sum_{i=0}^{k-1} \mathbf{HF}^i\mathbf{G} \end{bmatrix}, \mathbf{U} = \mathbf{u}_{0-k}, \quad \mathbf{u}_{0-k} = \mathbf{u}_0 = \mathbf{u}_k \tag{10}$$

where $\mathbf{u}_k \in \mathbb{R}^{n_i}$ is a vector of constant input forces between e.g. time-steps 0 and *k*. This situation offers the advantage of drastically increasing the redundancy of the problem to be solved and will be used later in this work to investigate the influence of increasing the horizon for input estimation.

2.2 Augmented Kalman Filter

If inputs are assumed to be known, a linear Kalman filter [11] can be directly applied to a system like the one of Eq.(6). By introducing the following so-called zero$^{\text{th}}$-order random walk model for the input [12] [8] [13]:

$$\dot{\mathbf{u}}(t) = \mathbf{0} + \mathbf{w}_u(t) \tag{11}$$

where $\mathbf{w}_u$ is a stochastic process with associated covariance matrix $\mathbf{Q}_u$, by inserting Eq.(11) into Eq.(6), by rearranging the system and finally discretizing it one obtains the equations of motion in state space and the discrete measurement equations (see e.g. [14] [9])

$$\begin{cases} \mathbf{x}_k^* &= \mathbf{F}^*\mathbf{x}_{k-1}^* + \mathbf{w}_{k-1} \\ \mathbf{y}_k &= \mathbf{H}^*\mathbf{x}_k^* + \mathbf{v}_k \end{cases} \tag{12}$$

where the augmented state vector is defined as

$$\mathbf{x}_k^* = \begin{bmatrix} \mathbf{x}_k \\ \mathbf{u}_k \end{bmatrix}. \tag{13}$$

Vectors $\mathbf{w}$ and $\mathbf{v}$, are not included in the standard definition of the equations of motion. They are the so-called process and measurement noise and represent random processes that are introduced in order to account for model and measurement uncertainties. The model is hence completely defined when also the covariance matrices $\mathbf{Q}$ and $\mathbf{R}$, associated with $\mathbf{w}$ and $\mathbf{v}$ respectively, are assigned. Note that the model given by Eq.(11) states that the rate of change of the force with respect to time can vary randomly. Given the form of Eq.(12), a linear Kalman filter can be applied to the system with augmented states hence leading to the simultaneous estimation of the states and the input of the system. Eq.(12) provides a state vector estimate $\hat{\mathbf{x}}_k^*$ at time step k. The a-priori $(\hat{\mathbf{x}}_k^{*-})$ and a-posteriori $(\hat{\mathbf{x}}_k^{*+})$ estimates are easily obtained in the following way [15]:

Time update

$$\hat{\mathbf{x}}_k^{*-} = \mathbf{F}^*\hat{\mathbf{x}}_{k-1}^{*+} \tag{14}$$

$$\mathbf{P}_k^- = \mathbf{F}^*\mathbf{P}_{k-1}^+\mathbf{F}^{*T} + \mathbf{Q}_{k-1}^* \tag{15}$$

Measurement update

$$\mathbf{K}_k = \mathbf{P}_k^-\mathbf{H}^{*T}\left(\mathbf{H}^*\mathbf{P}_k^-\mathbf{H}^{*T} + \mathbf{R}_k\right)^{-1} \tag{16}$$

$$\hat{\mathbf{x}}_k^{*+} = \hat{\mathbf{x}}_k^{*-} + \mathbf{K}_k\left(\mathbf{y}_k - \mathbf{H}^*\hat{\mathbf{x}}_k^{*-}\right) \tag{17}$$

$$\mathbf{P}_k^+ = (\mathbf{I} - \mathbf{K}_k \mathbf{H}^*)\, \mathbf{P}_k^- . \tag{18}$$

This is an unbiased linear state estimator designed to be optimal in the sense that it minimizes the trace of the error covariance matrix, defined as

$$\mathbf{P}_k = \mathbf{E}\left[(\mathbf{x}_k^* - \hat{\mathbf{x}}_k^*)\, (\mathbf{x}_k^* - \hat{\mathbf{x}}_k^*)^T \right], \tag{19}$$

where $\mathbf{P}_k^-$ is the *a-priori* error covariance matrix and $\mathbf{P}_k^+$ is the *a-posteriori* error covariance matrix. The noise processes $\mathbf{w}_k^*$ and $\mathbf{v}_k$ are assumed to be white, zero-mean and uncorrelated.
As already previously mentioned, since the augmented state vector $\mathbf{x}^*$ contains the unknown inputs, a coupled state-input estimation is effectively performed when Eqs.(14)-(18) are computed in each time step. In order to have a stable estimator it is required that the augmented system of Eq.(12) is observable. By definition, a discrete-time system like the one of Eq.(12) is said to be observable if for any initial state and for some final time step k, the initial state can be uniquely determined by knowledge of the output for all the time steps up to k [15]. By considering observability for structural systems, some theoretical requirements can be defined [8] [13]:

- the number of DOFs of the reduced model represented by Eq.(4) should be equal or greater than the number of forces to be estimated, i.e. $n_{red} \geq n_F$.
- the number of independent position level measurements (e.g. position or strain measurements) should be equal or greater than the number of forces to be estimated, i.e. $n_{plmeas} \geq n_F$.

2.3 Augmented Kalman Smoother

Given the fact that the main focus of this work is towards input-estimation and considering that forces applied to a dynamic system at time-step *k* cause changes in states only starting from time-step *k+1* (if position and strain measurements are to be used), an alternative to the AKF is also used. Namely a fixed-lag Augmented Kalman Smoother (AKS) is implemented following the algorithm presented in [15] (Chapter 9.3). Due to space limitations, the implementation details are not reported here. It suffices to say that a fixed lag smoother is used to obtain an estimate at time-step *k-N* using measurements up to and including time-step *k* (future measurements).

The smoother has the advantage that information on states captured at time-step *k* but caused by e.g. an input applied at time-step *k-N* can be included in the filter in order to enrich the amount of information related to the input. In particular the standard AKF tend to be *sluggish* and presents some sort of delay in the input estimates when not enough information to retrieve the input values is contained in measurements up to time *k-N*.

The disadvantages of the AKS are twofold: it is computationally more expensive and it provides an updated estimate of smoothed states/input at time-step *k* only after *N* time-steps. Both these disadvantages are not relevant for this work since real-time is not necessary and the computational burden is anyhow very limited thanks to the reduced size of the model (see Eq.4).

3 Ill conditioning and ill-posedness: numerical study

The test-case used during this work is a twistbeam rear suspension. Figure 1 shows a picture of the physical setup of the twistbeam and its FE model representation. The twistbeam is actuated thanks to a displacement input applied at the tyre patch while forces and torques are measured at the interface between the rim and the twistbeam. The work performed on the same setup and reported in [16] showed promising results for input estimation of a single vertical force. An extension of the work for multiple force estimation using real

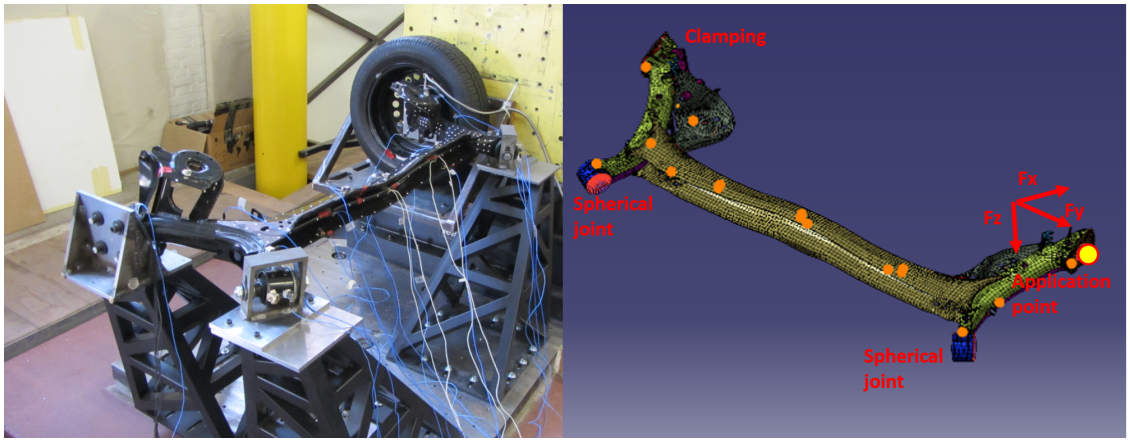

Figure 1: Twistbeam test-rig and FE model

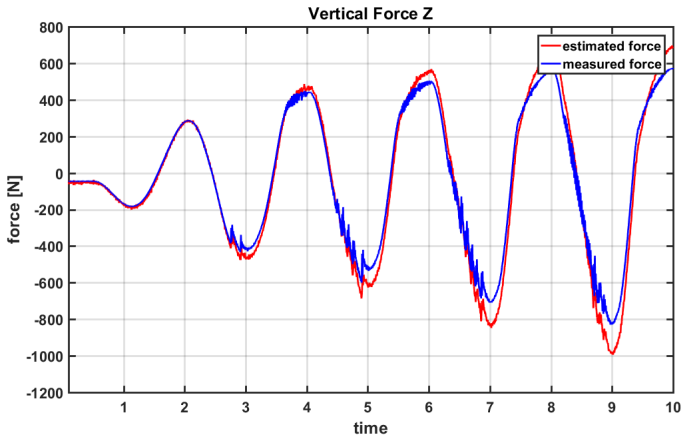

Figure 2: single force estimation - AKF experimental validation

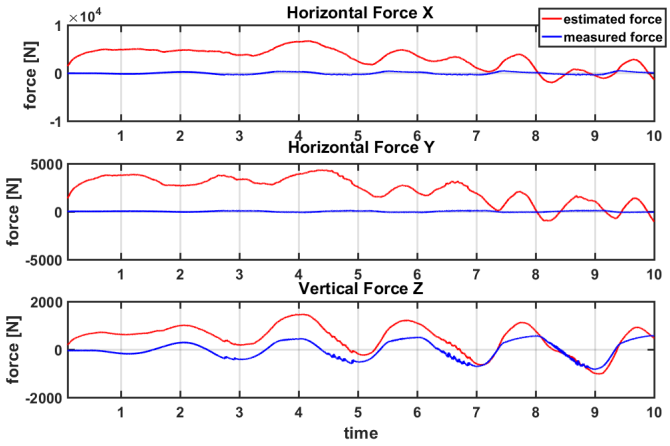

Figure 3: multiple force estimation - AKF experimental validation

measurements and a model of the twistbeam has been tried. Results for a low frequency sinusoidal input at the tyre patch are shown in Fig.2 - 3. It is clearly visible that single force estimation is performed very accurately while results are drastically inaccurate from the moment in which multiple forces are estimated. Interestingly, estimated measurements maintain instead a very good level of accuracy (see Fig.4).

In order to further understand the reasons of the previous problematic observations the current work started

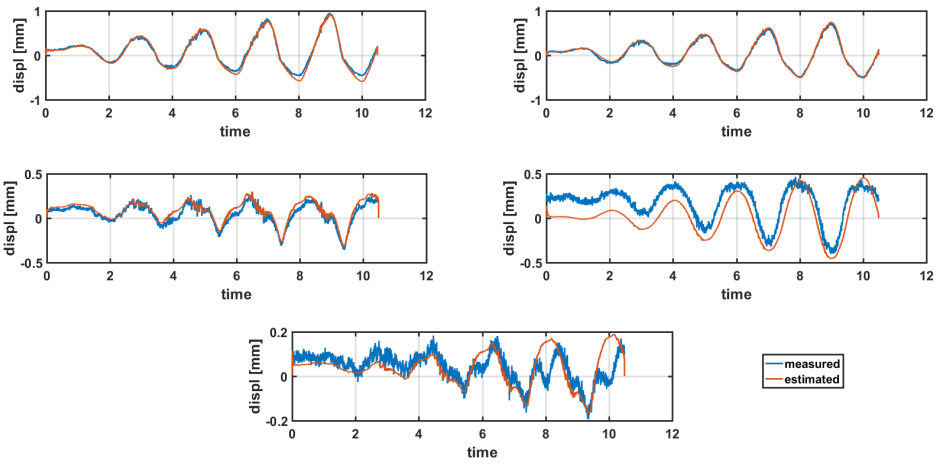

Figure 4: Estimated positions

by searching simple and clear explanations in the quest for pragmatic solutions. The main causes of the observed behavior can be categorized as follows:

- **Ill-conditioning**: As common in many (if not all) mechanical components, applying forces to the twistbeam at the input location along different directions, results in very different deformed shapes. This is caused by the different *stiffness* distribution of the structure along different directions. In layman's terms, a unit vertical load applied to the twistbeam z direction results in a much larger deformation as compared to a load applied e.g. along the y direction (see Fig.1). Table 1 gives an indication of the *driving point* static stiffness variation along different directions. It can be seen that a large ratio is obtained between K_y and K_z. This fact translates directly into an ill-conditioned inverse problem. As a consequence, noise present in measurements will be highly amplified during the matrix inversions involved in any of the used algorithms for input estimation.

- **Ill-posedness**: Several tests failed also when reconstructing only two forces (namely F_z and F_x) despite their seemingly low stiffness ratio. This behavior is caused by the ill-posedness of the problem. Due to the configuration of the twistbeam, loads applied along either the x or the z directions lead to almost the same (scaled) deformation and related strain field (see Fig.5). For this reason it is intuitive to understand that any estimator that uses position and strain measurements would not be able to distinguish between deformation caused by an input force applied along any of the two directions. As a result an infinite amount of combinations of z and x forces would allow to properly match the measurements (e.g. in a LLS sense) by applying completely unphysical forces.

- **states vs. input estimation**: Finally despite the ill-conditioning and ill-posedness of the problem, it was experimentally seen that quantities that are directly linked to system states can be correctly estimated, at measurement locations that are not used for the estimation itself and despite the very poor quality of the estimated input. This fact can be easily understood: if the used FE model is for example too stiff as compared to a real system (e.g. a too large Young modulus is used) forces would be wrongly estimated since the model is the only link between the measurements and the input forces (provided that no force measurements are used for the estimation). If the mass distribution and the stiffness distribution of the *wrongly-updated* model are instead in the correct ratios, eigenmodes and static deformation will have shapes that very similar to the ones of the real system. Basically, despite a poor model updating, the physics of the problem is still well captured. This fact will allow a proper estimation of the distributed fields despite a poor input estimation and is, to the authors judgment, a very important feature of the virtual sensing and state estimation using reduced FE-based models.

Static Stiffness $K_x\ [N/mm]$	**Static Stiffness** $K_y\ [N/mm]$	**Static Stiffness** $K_z\ [N/mm]$
1000	5000	27
Ratio K_x/K_z	**Ratio** K_y/K_z	-
37	185	-

Table 1: Static stiffness of twistbeam

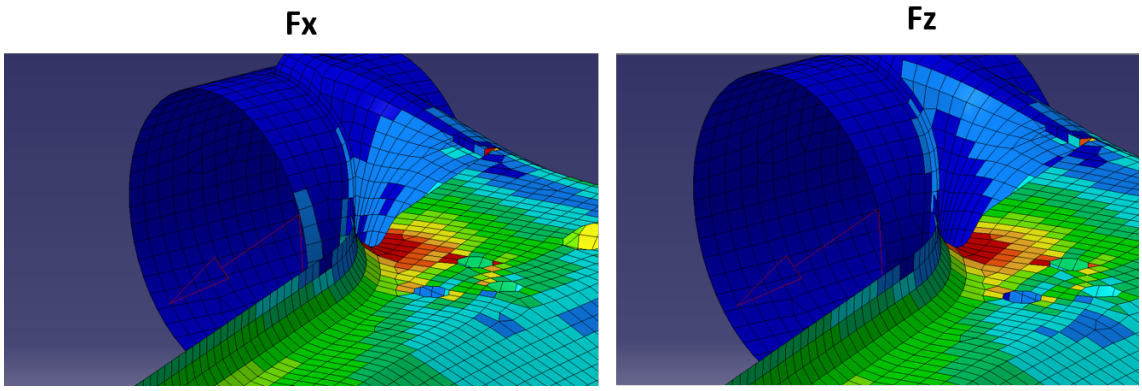

Figure 5: Strain Field for vertical and horizontal forces

4 Analysis of countermeasures based on LSS

Given the fact that ill-conditioning and ill-posedness cannot be completely removed since they represent characteristics that are mainly inherent to the nature of the structure under analysis, it was decided to perform at first a study on the influence of several parameters that might help reducing the above mentioned issues. It has to be noticed that in model-based inverse problems, the only link between the estimated input forces and the measurements (excluding direct or indirect force measurements) is the model itself. It goes without saying that an accurate model is of paramount importance especially in ill-posed/ill-conditioned problems. For this reason the remaining of the work uses an *"exact model"*: any of the *"measured"* quantities is synthesized from simulating the reduced FE model and by adding zero-mean uncorrelated Gaussian noise. The interesting question related to the influence of model accuracy on the estimation goes beyond the scope of this work.

At first a simple test is performed in order to study the influence of *estimation horizon*, *sensor noise* and *number of sensors* on the estimated forces. The LLS framework described in section 2.1 is used. In order to simplify the study three constant forces of different amplitudes are applied to the application point of the twistbeam. Some of the characteristics of the model and the simulations are provided in Table 2. The value for sensor noise is derived from the real available position sensors. The model is statically complete and the eigenmodes of the clamped structure are simply included in order to use the same model for the dynamic analysis performed in the following sections.

The main results of the parametric study are summarized in Figure 6. In particular the left figure shows the standard deviation of the error on F_x (which is the worst estimated force) in function of the amount

Number of nodes	34654
Element types	Nastran CQUAD, CTRIA, CTETRA
Number of included eigenmodes	10
Number of included attachment modes	3
Number of input	3
Static forces F_x, F_y, F_z **[N]**	100, 200, 1000
Reference pos. noise stdv	5.60E-05

Table 2: LLS Data

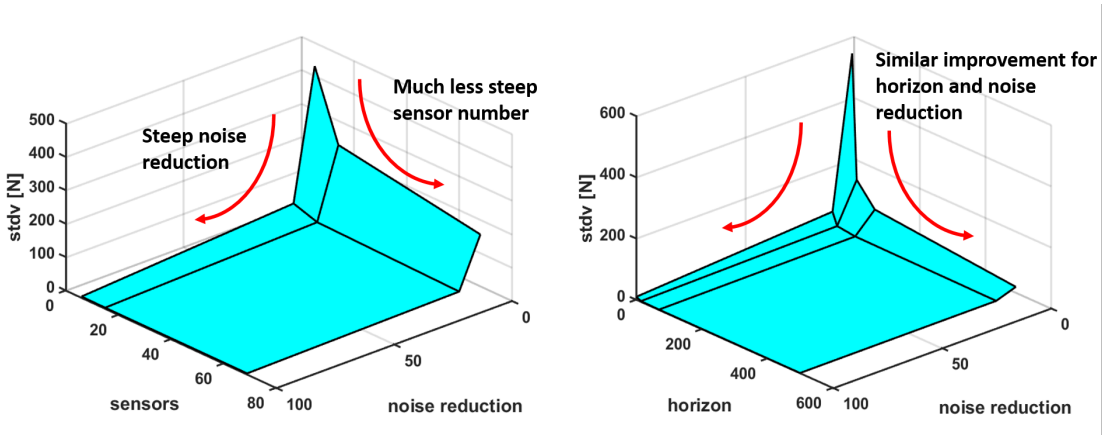

Figure 6: Influence of sensors accuracy, horizon and amount of sensors

of randomly located position sensors and reduction of noise - 10 representing a reduction of one order of magnitude with respect to the value reported in table 2 - . The right figure shows a similar plot in function of noise reduction and horizon length in time-steps. From this analysis it seems that reducing the noise (improving sensor quality) and increasing the estimation horizon leads to a significant improvement of the estimation. On the other hand, further reducing the noise level or increasing the horizon does not allow to obtain a proportionally better estimate and might not be worth the effort when considering the increased computational effort and the potential sensor cost involved. This result is to be expected since noise reduction means avoiding the cause of the problem while increasing the horizon allows to improve the conditioning of the LLS problem by using a largely overdetermined system of equations. Interestingly the estimation accuracy seems to be less influenced by the amount of sensors. It will be shown that this fact is due to the random nature of the selection performed for this test. It is indeed not important how many sensors are included but the amount of extra information that each sensor brings to the estimate. In simple terms if one would add sensors that are concentrated very close to each other the matrix $\mathbf{H}$ in Eq.7 would quickly become close to singular since all its rows will be almost linearly dependent.

The optimal sensors strategy developed in the next section will make use of the above mentioned physical observation. In particular, the noise influence will be reduced by selecting only highly excited locations, rank deficiency of matrix $\mathbf{H}$ will be reduced by selecting widely spread sensors and observability will be insured by maximizing an observability measure based on the PBH criterion (see e.g. [17], [18]).

5 Optimal sensor placement and other solutions for AKF

5.1 Optimal sensor placement

Following and partially extending the work presented in [18], we propose a pragmatic optimal sensor location strategy (see Fig.7) that allows to optimally (in a certain defined sense) define type and location of sensors to be used for input estimation in Kalman-based estimation. One key aspect of the strategy is related to the derivation of an observability measure. This observability measure is directly linked to the PBH criterion which states that $(\mathbf{A}, \mathbf{C})$ is observable if:

$$rank \begin{bmatrix} \mathbf{sI} - \mathbf{A} \\ \mathbf{C} \end{bmatrix} = rank(\mathbf{PBH}(\mathbf{s})) = \mathbf{n}, \quad \forall \mathbf{s} \in \mathbb{C} \tag{20}$$

where $\mathbf{n}$ is the size of the square matrix $\mathbf{A}$. For structural dynamics application with random walks and if $\mathbf{C}=\mathbf{0}$, the PBH matrix becomes rank deficient when evaluated at the eigenvalues of matrix $\mathbf{A}$ With an eye towards input estimation and random walk force models it can be easily noticed that the eigenvalues related to the random walk eigenvectors are at $0\,[Hz]$. Keeping in mind that:

- The primary goal of this work is to obtain reliable input estimation;
- Structural modes that are not observable are anyhow detectable if the system is damped and lead to a stable estimation;
- Numerically, the PBH matrix will never be rank deficient but its condition number is a good measure for being *close-to-singularity*;

it is possible to define the following observability measure:

$$\mathbf{O}_m = \frac{1}{\mathbf{n}_i \cdot cond(\mathbf{PBH}(0))}, \tag{21}$$

where n_i is the number of input to be estimated. After the definition in Eq.21 the following optimal sensor placement strategy is implemented:

- **Pool of sensors**: Initialize the algorithm by selecting a large pool of sensors spread randomly over the FE model. This pool of sensors should include position, strain and acceleration sensors when possible. The algorithm is optimal for the FE model only if the pool of sensors includes all the available FE nodes. Otherwise the algorithm is sub-optimal with respect to all the potential sensor locations and optimal with respect to the initial pool - but it can be extremely beneficial nonetheless;
- **Instantiate training scenarios**: Simulate the reduced numerical model for a series of training scenarios. In the current work, training scenarios include sinusoidal excitations at different frequencies (in the expected excitation frequency range) for each input location and direction;
- **Coarse screening**: In order to avoid using sensors with low signal-to-noise ratio, only the sensors that have the maximum output amplitude during training are selected. In this stage, a maximum number of sensors per training scenarios is selected. This is repeated for all the different sensors type present. Moreover, each sensor location (per sensor type) should respect a distance metric. Namely, two sensors of the same type and measuring along the same direction should not be closer than a certain user-defined distance. In this way the measurement equations will remain as linearly independent as possible;
- **Merge sensors and scaling**: In this stage, the remaining sensors per each training scenarios are merged, duplicated sensors are removed and the rows of the measurement matrix $\mathbf{C}$ are scaled to have a maximum unity value. In this way, the PBH criterion will not privilege one sensor type with respect to another simply due to e.g. unit scaling.
- **Observability screening**: At first, the current observability measure $\mathbf{O}_m$ is evaluated for the remaining sensors. This value is stored as allows to have a reference for observability. It is assumed that given the large amount of sensors still remaining, the system is fully observable. In this stage, a loop is performed for the remaining sensors. During each loop each of the remaining sensors is sequentially removed from the measurement equation. A new observability measure (without the current sensor) is computed and stored. At the end of each loop, the sensor corresponding to a minimum decrease in the observability measure is removed from the sensor pool. In this way, the most redundant sensor is eliminated in a greedy fashion [19]. The loop continue until the maximum amount of sensors available is reached.

This (sub) optimal scheme was applied to several scenarios and proved to be robust in all the tested conditions. The *Observability screening* can be computationally expensive due its factorial nature. A preliminary extension of strategy for non-linear systems has been proposed in [18].

Figure 8 visually shows two sensors configurations obtained using the optimal sensor placement strategy (left) and a random sensor selection. It can be seen that while the random selection locates only a few sensors

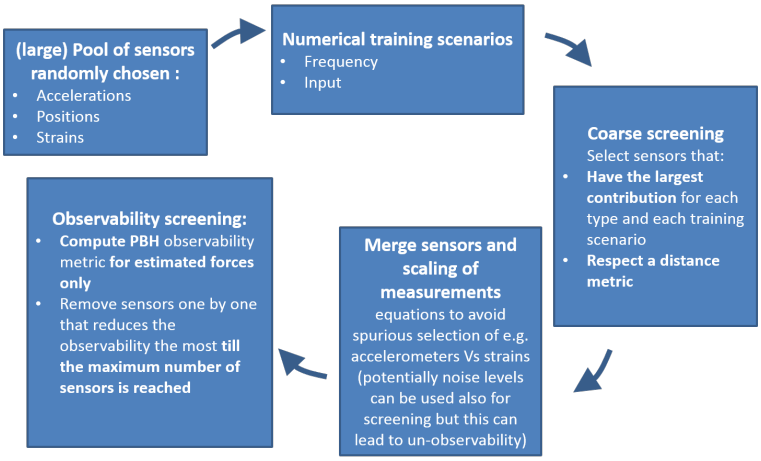

Figure 7: Optimal sensor placement strategy

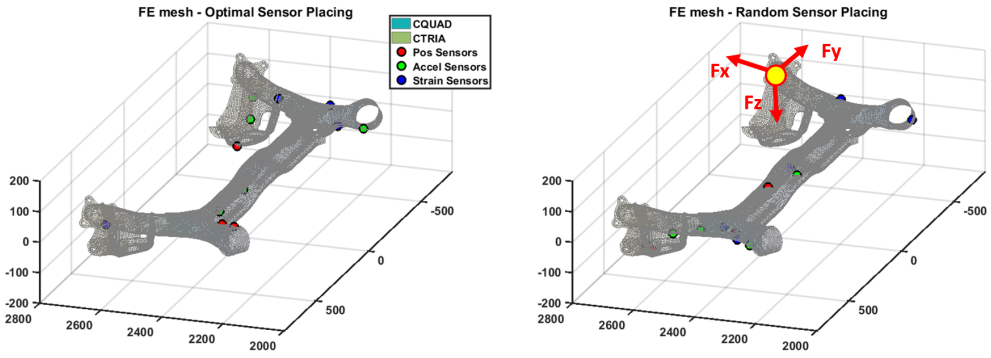

Figure 8: Optimal Vs Random sensor distribution

close to the input application point, the optimal sensors placement locates the sensors in a way which can be easily explained from a physical point of view. At least one position sensor is placed in a location where large deformation are expected, the other position sensors are located close to a clamping area where large reaction forces are expected to enter the system. Almost all the strain sensors are located close to clamping locations where deformation gradients are larger. Finally more than three (number of input forces) position or strain sensors are selected. It has to be underlined that this explanation holds for linear systems and quasi-static conditions. More complex scenarios are not that straightforward to analyze. Nonetheless this intuitive behavior allows to increase confidence in the algorithm.

5.2 Numerical results

The presented strategy is applied to series of simulations in which AKFs and AKSs are applied. Table 3 provides the details of the simulations but similar results have been obtained in different cases (e.g. simulated road input or results in [20]). The values for the model error covariance used for the Kalman filter random-walk model have been estimated by assuming the order of magnitude of the input force and estimating a maximum frequency of interest. Figure 9 shows the input estimation results obtained for three input forces. The notation *reduced noise*, stands for a reduction of one order of magnitude with respect to the values reported in table 3. As it can be seen the force estimation with noise taken from standard sensor values is not successful for input along the *"stiff"* directions. This is true regardless the optimal sensor placement. This is already a very valuable information since it directly allows to avoid useless measurement campaigns when a satisfactory result cannot be achieved. Things do not seem to drastically improve when a lower noise is used (e.g. using more expensive sensors) if sensors are randomly located. Finally the optimal sensor placement

Simulation Data	Value
Simulation time [s]	2
Time step [s]	1.0E-03
Input frequency [Hz]	5
Input type	DC+ramp+sine
Ramp time [s]	1
DC Force component F_x, F_y, F_z [N]	200, 500, 500
Sinusoidal Force component F_x, F_y, F_z [N]	200, 200, 1000
Estimation Data	**Value**
Pos. noise stdv [mm]	5.6E-05
Strain. noise stdv [mm/mm]	0.33
Acceleration noise stdv [mm/s^2]	2500
Optimal Sensor Placement Data	**Value**
Initial pool of sensors	9000
Maximum number of sensros per training scenario	50
Maximum number of sensors	15
Maximum distance between sensors [mm]	150
Training frequencies [Hz]	0, 10, 20

Table 3: Simulatiom, estimation and sensor placement data

strategy allows to obtain a significantly improved input estimation. This is obtained thanks to the fact that the 15 selected sensors allow to achieve a reduction of the observability measure of only 30% with respect to what available after the *Coarse screening* (over 200 sensors).

Figure 10 shows the improvement in estimation results with 45 optimally selected sensors. This still leads to a significant estimation improvements. The decrease in observability measure is in this case only 15%. Finally Fig.11 shows an example (on a low frequency test-case) of the estimation results obtained with a Kalman smoother that has a fixed lag of 300 t-steps. As expected, that the smoother results better preserve the phase of the original input and lower the amount of noise on the estimate. Despite this result, it was found that improvements due to smoothing are limited for the twistbeam case.

6 Conclusions

In this work, an engineering approach to states-input estimation of linear structural dynamics systems is proposed. In order to perform a reliable force estimation, it is of paramount importance to:

- Use a properly updated numerical model. States can be properly captured even with non updated model provided that the physics of the system is well captured;
- Increase the signal-to-noise ratio as much as possible by using accurate sensors and/or properly selecting their location;
- Properly assess the *level of observability* of your system by using e.g. an observability measure;
- Use a limited but well placed amount of sensors;

Future research will concentrate in studying the usage of novel sensor types for input estimation and into validating the proposed optimal sensor strategy on non-linear systems

Acknowledgements

The authors gratefully acknowledge the VLAIO (Flemish Innovation & Entrepreneurship) through its Innovation mandate IWT project VIRTUAL MATES (nr. 140778), the European Commission for its support of

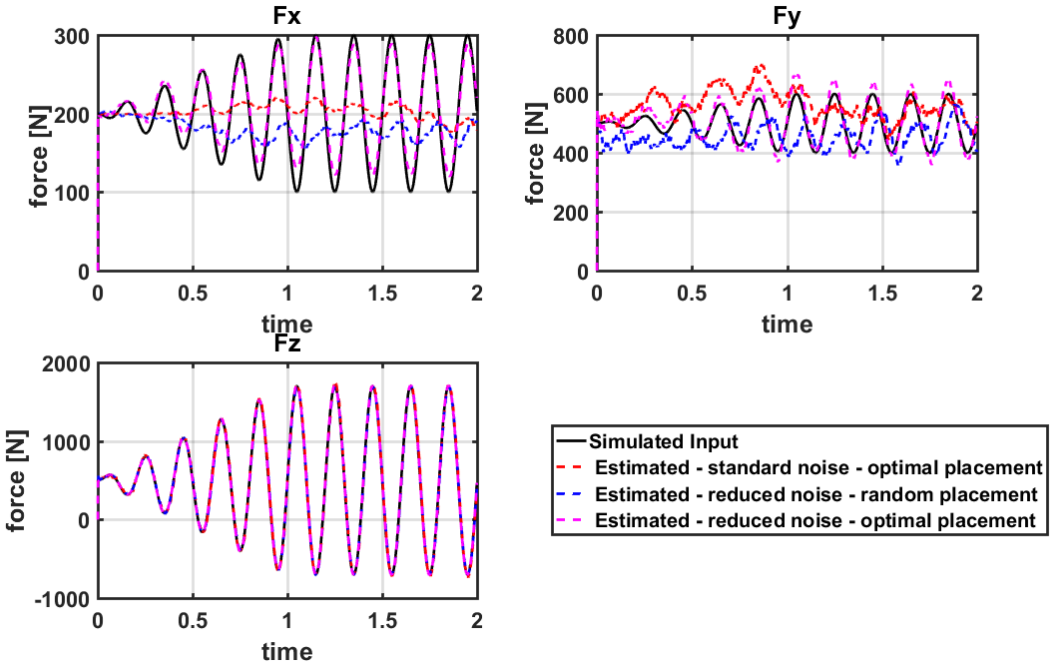

Figure 9: Force estimation - optimal sensors placement and noise

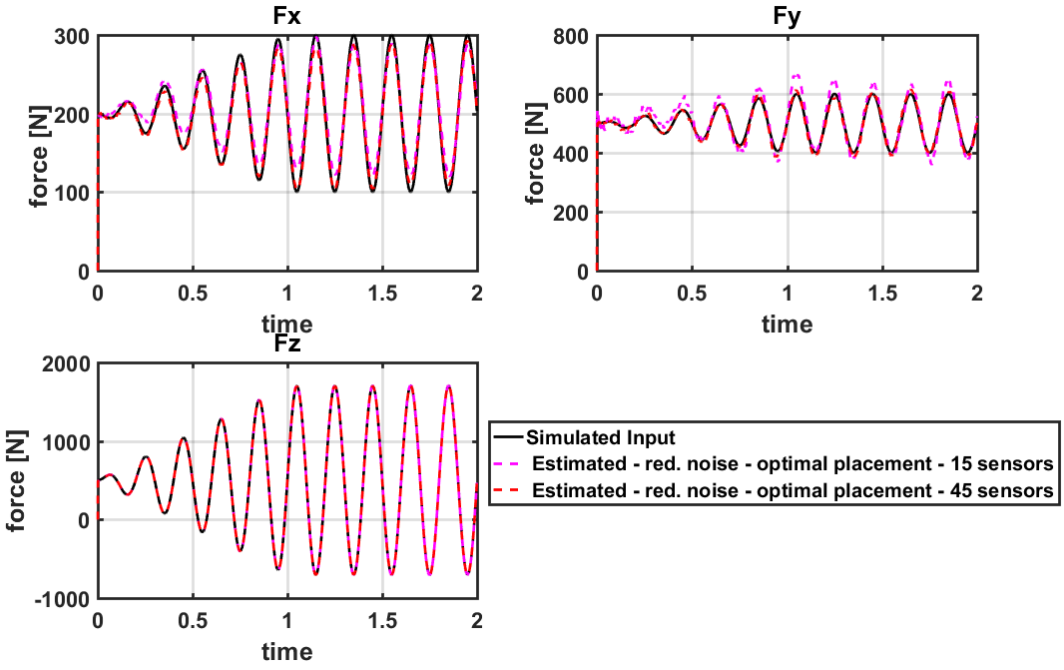

Figure 10: Force estimation - increasing observability

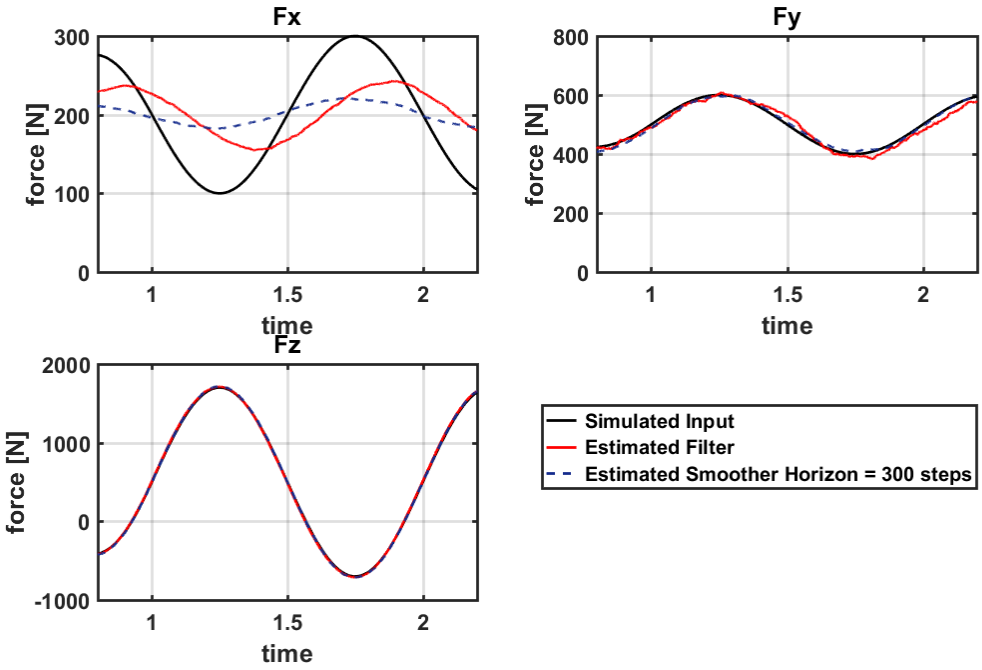

Figure 11: Force estimation effect of horizon

the Marie Sklodowska Curie program through the ITN ANTARES project (GA 606817) and the Research Fund KU Leuven. The research of W. Rottiers is funded by a grant from the Fund fr Scientific Research -Flanders (F.W.O). This research was partially supported by Flanders Make.

References

[1] R. Adams, J. F. Doyle, *Multiple force identification for complex structures*, Experimental Mechanics, Vol. 42, No. 1, (2002), pp. 25–36.

[2] C.-K. Ma, J.-M. Chang, D.-C. Lin, *Input forces estimation of beam structures by an inverse method*, Journal of sound and vibration, Vol. 259, No. 2, (2003), pp. 387–407.

[3] H. Choi, A. Thite, D. Thompson, *A threshold for the use of tikhonov regularization in inverse force determination*, Applied Acoustics, Vol. 67, No. 7, (2006), pp. 700–719.

[4] M. V. van der Seijs, D. de Klerk, D. J. Rixen, *General framework for transfer path analysis: History, theory and classification of techniques*, Mechanical Systems and Signal Processing, Vol. 68, (2016), pp. 217–244.

[5] O. C. Zienkiewicz, R. L. Taylor, *The finite element method*, Butterworth Heinemann, Oxford (2000).

[6] B. Besselink, U. Tabak, A. Lutowska, N. van de Wouw, H. Nijmeijer, D. J. Rixen, M. E. Hochstenbach, W. H. A. Schilders, *A comparison of model reduction techniques from structural dynamics, numerical mathematics and system and control*, Journal of Sound and Vibration, Vol. 332, (2013), pp. 4403–4422.

[7] R. R. Craig, *A review of time-domain and frequency domain component mode synthesis methods*, Journal of Modal Analysis 2, Vol. 2, No. 2, (1987), pp. 59–72.

[8] F. Naets, J. Cuadrado, W. Desmet, *Stable force identification in structural dynamics using* K*alman filtering and dummy-measurements*, Mechanical Systems and Signal Processing, Vol. 50-51, (2015), pp. 235–248.

[9] C. F. V. Loan, *Computing integrals involving the matrix exponential*, IEEE Transactions on Automatic Control, Vol. 23, No. 3, (1978), pp. 395–404.

[10] T. Uhl, *The inverse identification problem and its technical application*, Archive of Applied Mechanics, Vol. 77, No. 5, (2007), pp. 325–337.

[11] R. Kalman, *A new approach to linear filtering and prediction problems*, Journal of Basic Engineering, Vol. 82, No. 1, (1960), pp. 35–45.

[12] E. Lourens, E. Reynders, G. D. Roeck, G. Degrande, G. Lombaert, *An augmented* K*alman filter for force identification in structural dynamics*, Mechanical Systems and Signal Processing, Vol. 27, (2012), pp. 446–460.

[13] F. Naets, J. Croes, W. Desmet, *An online coupled state/input/parameter estimation approach for structural dynamics*, Computer Methods in Applied Mechanics and Engineering, Vol. 283, (2015), pp. 1167–1188.

[14] E. Risaliti, B. Cornelis, T. Tamarozzi, W. Desmet, *A state-input estimation approach for force identification on an automotive suspension component*, *34th International Modal Analysis Conference (IMAC34)*, Orlando, Florida.

[15] D. Simon, *Optimal state estimation: Kalman, H_∞ and nonlinear approaches*, John Wiley, New York (2006).

[16] F. Cosco, F. Naets, W. Desmet, *Use of concept modelling for online input force estimation*, *In International Conference on Noise and Vibration Engineering (ISMA2014)*.

[17] B. K. Ghosh, J. Rosenthal, *et al.*, *A generalized popov-belevitch-hautus test of observability*, IEEE transactions on automatic control, Vol. 40, No. 1, (1995), pp. 176–180.

[18] W. Rottiers, *Development of virtual measurements on a mechatronic drivetrain*, *Master thesis, KU Leuven (2015)*, Belgium.

[19] N. P. Salau, J. O. Trierweiler, A. R. Secchi, *Observability analysis and model formulation for nonlinear state estimation*, Applied Mathematical Modelling, Vol. 38, No. 23, (2014), pp. 5407–5420.

[20] E. Risaliti, J. V. Cauteren, T. Tamarozzi, B. Cornelis, W. Desmet, *Virtual sensing of wheel center forces by means of a linear state estimator*, *In International Conference on Noise and Vibration Engineering (ISMA2016)*, Leuven, Belgium,.